JOC Article

Synthesis of Covalently Linked Unsymmetrical Porphyrin Pentads Containing Three Different Porphyrin Subunits

Smita Rai and Mangalampalli Ravikanth*

Department of Chemistry, Indian Institute of Technology, Bombay, Powai, Mumbai 400 076, India

ravikanth@chem.iitb.ac.in

Received July 4, 2008

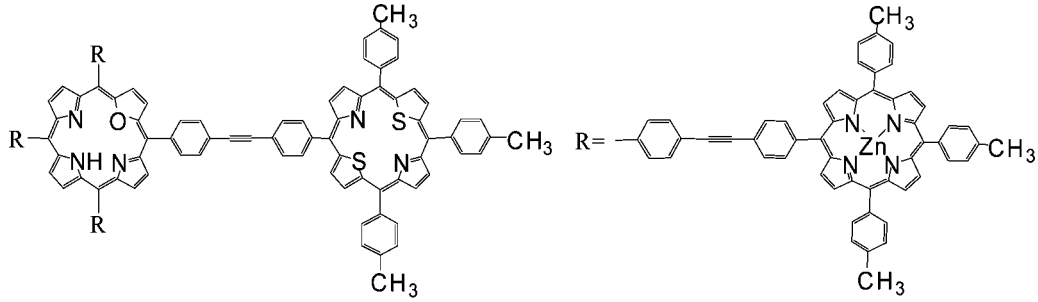

The tetrafunctionalized AB_3-type porphyrin building blocks containing two different types of functional groups with N_4, N_3O, N_3S, and N_2S_2 porphyrin cores were synthesized by following various synthetic routes. The AB_3-type tetrafunctionalized N_4 porphyrin building block was synthesized by a mixed condensation approach, the N_3S and N_3O porphyrin building blocks by a mono-ol method, and N_2S_2 porphyrin building block by an unsymmetrical diol method. The tetrafunctionalized porphyrin building blocks were used to synthesize monofunctionalized porphyrin tetrads containing two different types of porphyrin subunits by coupling of 1 equiv of tetrafunctionalized N_4, N_3O, N_3S, and N_2S_2 porphyrin building block with 3 equiv of monofunctionalized ZnN_4 porphyrin building block under mild copper-free Pd(0) coupling conditions. The monofunctionalized porphyrin tetrads were used further to synthesize unsymmetrical porphyrin pentads containing three different types of porphyrin subunits by coupling 1 equiv of monofunctionalized porphyrin tetrad with 1 equiv of monofunctionalized N_2S_2 porphyrin building blocks under the same mild Pd(0) coupling conditions. The NMR, absorption, and electrochemical studies on porphyrin tetrads and porphyrin pentads indicated that the monomeric porphyrin subunits in tetrads and pentads retain their individual characteristic features and exhibit weak interaction among the porphyrin subunits. The steady state and time-resolved fluorescence studies support an efficient energy transfer from donor porphyrin subunit to acceptor porphyrin subunit in unsymmetrical porphyrin tetrads and porphyrin pentads.

Introduction

Natural photosynthetic systems employ elaborate light-harvesting complexes to capture dilute sunlight and funnel the captured energy to the reaction center through rapid and efficient transfer processes.[1] A major objective in the field of artificial photosynthesis is to create synthetic light-harvesting complexes. In recent times, several covalently linked multiporphyrin arrays have been synthesized and their excited-state properties have been explored to understand not only the light-harvesting properties of the photosynthesis reaction center but also their use for various other applications.[2] A common feature among the various multiporphyrin arrays reported in the literature is

(1) (a) McDermott, G.; Prince, S. M.; Freer, A. A.; Hawthornthwaite-Lawless, A. M.; Papiz, M. Z.; Cogdell, R. J.; Isaacs, N. W. *Nature* **1995**, *374*, 517. (b) Koepke, J.; Hu, X.; Muenke, C.; Schulten, K.; Michel, H. *Structure* **1996**, *4*, 581. (c) Pullerits, T.; Sundstrom, V. *Acc. Chem. Res.* **1996**, *29*, 381.

(2) (a) Wagner, R. W.; Seth, J.; Yang, S.-I.; Kim, D.; Bocian, D. F.; Holten, D.; Lindsey, J. S. *J. Org. Chem.* **1998**, *63*, 5042. (b) Li, J.; Ambroise, A.; Yang, S.-I.; Diers, J. R.; Seth, J.; Wack, C. R.; Bocian, D. F.; Holten, D.; Lindsey, J. S. *J. Am. Chem. Soc.* **1999**, *121*, 8927. (c) Song, H.-E.; Kirmaier, C.; Schwartz, J. K.; Hindin, E.; Yu, L.; Bocian, D. F.; Lindsey, J. S.; Holten, D. *J. Phys. Chem. B* **2006**, *110*, 19131. (d) Biemans, H. A. M.; Rowa, A. E.; Verhoeven, A.; Vanoppen, P.; Latterini, L.; Foekema, J.; Schenning, A. P. H. J.; Meijer, E. W.; de Schryver, F. C.; Nolte, R. J. M. *J. Am. Chem. Soc.* **1998**, *120*, 11054. (e) Sugiura, K.; Fujimoto, Y.; Sakata, Y. *Chem. Commun.* **2000**, 1105. (f) Cho, H. S.; Rhee, H.; Song, J. K.; Min, C.-K.; Takase, M.; Aratani, N.; Cho, S.; Osuka, A.; Joo, T.; Kim, D. *J. Am. Chem. Soc.* **2003**, *125*, 5849. (g) Shoji, O.; Okada, S.; Satake, A.; Kobuke, Y. *J. Am. Chem. Soc.* **2005**, *127*, 2201.

10.1021/jo801455w CCC: $40.75
Published on Web 10/02/2008

that they invariably contain similar porphyrin cores (N_4). The energy transfer properties of such symmetrical porphyrin arrays containing N_4 porphyrin cores have been studied by creating an energy gradient between the two porphyrin subunits by insertion of a metal such as Zn(II), Mg(II), and Sn(II) in the one of the porphyrin subunits and leaving the other porphyrin subunit in the free base form.[3] Thus, porphyrin arrays like star-shaped porphyrin pentads[4] containing four peripheral metalated porphyrin subunits and one central free base porphyrin subunit were synthesized. These systems act as a light-harvesting array containing multiple photoactive energy donors funnelling energy to one low lying energy acceptor. However, in these symmetrical porphyrin arrays, the absorption bands of metalated porphyrin may overlap with the free base porphyrin subunit of porphyrin arrays; hence, the selective excitation of donor porphyrin subunit is difficult. Furthermore, the emission bands of donor and acceptor porphyrin subunits also considerably overlap with each other which in some cases causes problem for accurate estimation of singlet−singlet energy-transfer parameters. To circumvent these problems, recently the efforts have been directed in design and synthesis of unsymmetrical arrays containing two different macrocycles such as porphyrin−chlorin,[5] porphyrin−corrole,[6] porphyrin−pheophorbide,[7] and porphyrin−phthalocyanine[8] macrocycles. These unsymmetrical arrays are useful to study singlet−singlet energy transfer and also to obtain fast initial charge transfer and a slow back reaction, thus giving a long-lived charge-transfer state.

We recently investigated the synthesis of a variety of β- and *meso*-substituted core-modified porphyrins to study their electronic properties.[9] The modification of porphyrin core by replacing one or two inner nitrogens with other heteroatoms such as sulfur, oxygen, selenium, and tellurium forms a group of core-modified porphyrins[10] containing different kinds of porphyrin cores such as N_3S, N_2S_2, N_3O, N_2SO, N_2OS, N_3Se, N_3Te, N_2Se_2, etc. The core-modified porphyrins exhibit interesting properties in terms of both aromatic character and their ability to stabilize metals in unusual oxidation states.[10] The electronic properties of core-modified porphyrins are quite different from normal porphyrins (N_4 core). An assembly of such core-modified porphyrin and normal porphyrin (N_4 core) or with any other macrocycle such as corrole, phthalocyanine, etc. would offer unique dyads or higher oligomers which are expected to have unusual electronic structure and interesting photophysical properties. Van Patten and co-workers[11] on the basis of computational studies predicted that a set of porphyrins such as N_4, N_3O, N_3S, N_2OS, and N_2S_2 porphyrins arranged in a linear series with a progressive decrease in energy levels could provide the basis for an energy cascade. We synthesized a series of unsymmetrical porphyrin dyads[12] containing two different macrocycles such as N_4-N_3O, N_4-N_3S, $N_4-N_2S_2$, N_3O-N_3S, $N_3S-N_2S_2$, etc., and preliminary photophysical studies supported an efficient energy transfer from one porphyrin subunit to another in these systems. However, except our own few examples of unsymmetrical porphyrin oligomers containing core-modified porphyrins, the reports on unsymmetrical porphyrin arrays containing core-modified porphyrin as one of the porphyrin subunit are almost scarce due to lack of proper synthetic methods to synthesize the functionalized core-modified porphyrin building blocks. Furthermore, the examples of covalently linked unsymmetrical arrays comprised of five or more macrocycles with two different macrocycles are very few in literature. Lindsey and co-workers synthesized multiporphyrin−phthalocyanine arrays such as pentads[8a] and nonads[8b] comprising four porphyrins and one phthalocyanine and eight porphyrins and one phthalocyanine, respectively, and demonstrated an efficient energy transfer from porphyrins to phthalocyanine in these novel systems (Chart 1). We synthesized unsymmetrical porphyrin pentad containing four peripheral N_4 porphyrin subunits and one central N_2S_2 porphyrin subunit and showed an efficient singlet−singlet energy transfer from peripheral N_4 porphyrin subunits to central N_2S_2 porphyrin subunit (Chart 1).[13] Recently, we also assembled three different types of porphyrin subunits using both covalent and noncovalent approaches (Chart 1).[14] Except for our one above-mentioned unsymmetrical porphyrin triad, to the best of our knowledge, there are no reports on unsymmetrical arrays containing more than two types of macrocycles. In this paper, we synthesized the new AB_3 type tetrafunctionalized porphyrins with N_4, N_3O, N_3S, and N_2S_2 cores by modifying the available methods. The tetrafunctionalized porphyrin building blocks were then used for the synthesis of four monofunctionalized porphyrin tetrads containing two different types of porphyrin subunits. In the last step, the monofunctionalized porphyrin tetrads were used to synthesize four unsymmetrical pentads containing three different types of porphyrins **1**−**4** (Chart 2). The preliminary photophysical studies on pentads **1**−**4** clearly demonstrated an energy transfer from three peripheral porphyrin subunits to central porphyrin subunit and then from the central porphyrin subunit to the other peripheral porphyrin subunit.

Results and Discussion

Synthesis of AB_3-Type Tetrafunctionalized Porphyrin Building Blocks. To synthesize covalently linked diphenyl ethyne-bridged unsymmetrical porphyrin pentads **1**−**4** containing three different types of porphyrin subunits (Chart 2), the AB_3 type of tetrafunctionalized porphyrin building blocks with

(3) (a) Holten, D.; Bocian, D. F.; Lindsey, J. S. *Acc. Chem. Res.* **2002**, *35*, 57. (b) Burrell, A. K.; Officer, D. L.; Plieger, P. G.; Reid, D. C. W. *Chem. Rev.* **2001**, *101*, 2751.

(4) (a) Prathapan, S.; Johnson, T. E.; Lindsey, J. S. *J. Am. Chem. Soc.* **1993**, *115*, 7519. (b) Seth, J.; Palaniappan, V.; Johnson, T. E.; Prathapan, S.; Lindsey, J. S. *J. Am. Chem. Soc.* **1994**, *116*, 10578.

(5) Arnold, D. P.; Hartnell, R. D. *Tetrahedron* **2001**, *57*, 1335.

(6) (a) Kadish, K. M.; Fremond, L.; Ou, Z.; Shao, J.; Shi, C.; Anson, F. C.; Burdet, F.; Gros, C. P.; Barbe, J. M.; Guilard, R. *J. Am. Chem. Soc.* **2005**, *127*, 5625. (b) Guilard, R.; Gros, C. P.; Barbe, J. M.; Espinosa, E.; Jerome, F.; Tabard, A. *Inorg. Chem.* **2004**, *43*, 7441. (c) Guilard, R.; Burdet, F.; Barbe, J. M.; Gros, C. P.; Espinosa, E.; Shao, J.; Ou, Z.; Zhan, R.; Kadish, K. M. *Inorg. Chem.* **2005**, *44*, 3972. (d) Kadish, K. M.; Shao, J.; Ou, Z.; Zhan, R.; Burdet, F.; Barbe, J. M.; Gros, C. P.; Guilard, R. *Inorg. Chem.* **2005**, *44*, 9023. (e) Kadish, K. M.; Shao, J.; Ou, Z.; Fremond, L.; Zhan, R.; Burdet, F.; Barbe, J. M.; Gros, C. P.; Guilard, R. *Inorg. Chem.* **2005**, *44*, 6744. (f) Gros, C. P.; Brisach, F.; Meristoudi, A.; Espinosa, E.; Guilard, R.; Harvey, P. D. *Inorg. Chem.* **2007**, *46*, 125.

(7) Shinoda, S.; Tsukube, H.; Nishimura, Y.; Yamazaki, I.; Osuka, A. *Tetrahedron.* **1997**, *53*, 13657.

(8) (a) Li, J.; Diers, J. R.; Seth, J.; Yang, S. I.; Bocian, D. F.; Holten, D.; Lindsey, J. S. *J. Am. Chem. Soc.* **1999**, *64*, 9090. (b) Li, J.; Lindsey, J. S. *J. Org. Chem.* **1999**, *64*, 9101. (c) Yang, S. I.; Li, J.; Cho, H. S.; Kim, D.; Bocian, D. F.; Holten, D.; Lindsey, J. S. *J. Mater. Chem.* **2000**, *10*, 283.

(9) Gupta, I.; Ravikanth, M. *Coord. Chem. Rev.* **2006**, *250*, 468.

(10) Latos-Grazynski, L. In *The Porphyrin Handbook*; Kadish, K. M.; Smith, K. M.; Guilard, R., Eds.; Academic Press: New York, 2000; Vol. 2, p 361.

(11) Van patten, P. G.; Shreve, A. P.; Lindsey, J. S.; Donhoe, R. J. *J. Phys. Chem. B* **1998**, *102*, 4209.

(12) (a) Punidha, S.; Ravikanth, M. *Tetrahedron* **2004**, *60*, 8437. (b) Gupta, I.; Ravikanth, M. *J. Org. Chem.* **2004**, *69*, 6796. (c) Punidha, S.; Agarwal, N.; Ravikanth, M. *Eur. J. Org. Chem.* **2005**, 2500. (d) Gupta, I.; Frohlich, R.; Ravikanth, M. *Chem. Commun.* **2006**, 3726. (e) Punidha, S.; Agarwal, N.; Gupta, I.; Ravikanth, M. *Eur. J. Org. Chem.* **2007**, 1168. (f) Rai, S.; Ravikanth, M. *Tetrahedron* **2007**, *11*, 2455.

(13) Kumaresan, D.; Agarwal, N.; Ravikanth, M. *J. Chem. Soc., Perkin Trans. 1* **2001**, 1644.

(14) Punidha, S.; Ravikanth, M. *Synlett* **2005**, *14*, 2199.

CHART 1. Structures of Unsymmetrical Porphyrin Arrays Containing More than One Type of Macrocycle

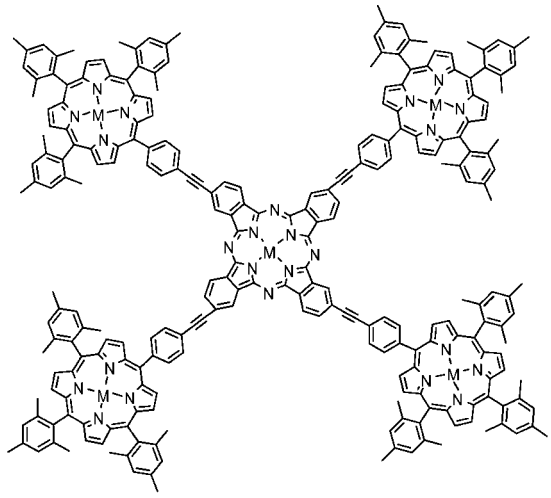

Unsymmetrical porphyrin-phthalocyanine pentad

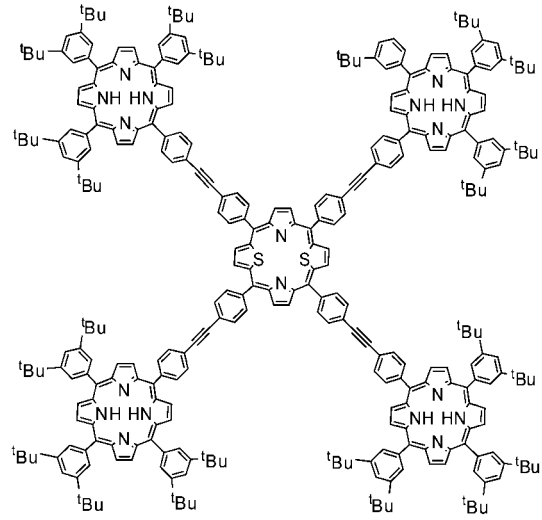

Unsymmetrical N_4-N_2S_2 porphyrin pentad

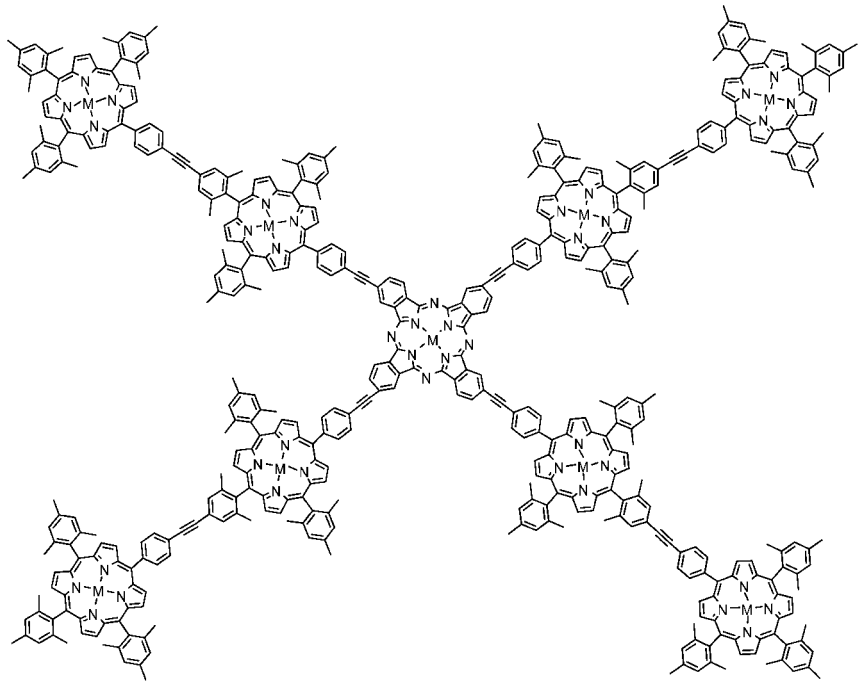

Unsymmetrical porphyrin-phthalocyanine nonad

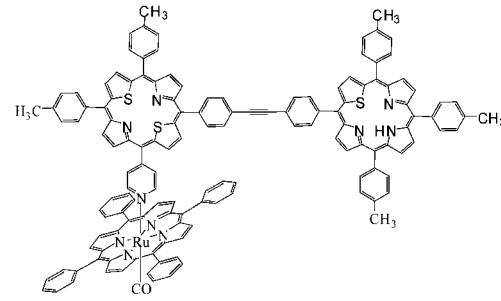

Unsymmetrical porphyrin triad

different cores such as N_4, N_3O, N_3S, and N_2S_2 are required. Since the diphenyl ethyne bridges were used to connect the porphyrin subunits, the porphyrin building blocks bearing functional groups such as iodophenyl and ethynylphenyl groups at *meso*-positions are required for Pd-mediated coupling reactions. The AB_3 type of *meso*-functionalized N_4 porphyrin building block **5** containing three iodophenyl groups and one protected ethynylphenyl group at the *meso* positions was synthesized by condensing 3 equiv of 4-iodobenzaldehyde with 1 equiv of 4-(3-hydroxy-3-methylbut-1-ynyl)benzaldehyde and 4 equiv of pyrrole in propionic acid at refluxing temperature for 3 h.[15] After standard workup and one filtration column on silica gel using dichloromethane as solvent, the TLC analysis showed the formation of statistical mixture of six porphyrins. The desired N_4 porphyrin building block **5** was separated from rest of the porphyrin mixture by silica gel column chromatography and isolated pure **5** as purple solid in 10% yield. However, to synthesize AB_3 type N_3O **6**, N_3S **7**, and N_2S_2 **8** porphyrin building blocks, there are no proper synthetic methods available in literature. Recently we developed mono-ol[12b] and unsym-

(15) Adler, A. D.; Longo, F. R.; Finarelli, J. D.; Goldmacher, J.; Assour, J.; Korsakoff, L. *J. Org. Chem.* **1967**, *32*, 476.

CHART 2. Unsymmetrical Porphyrin Pentads Containing Three Different Types of Porphyrin Subunits

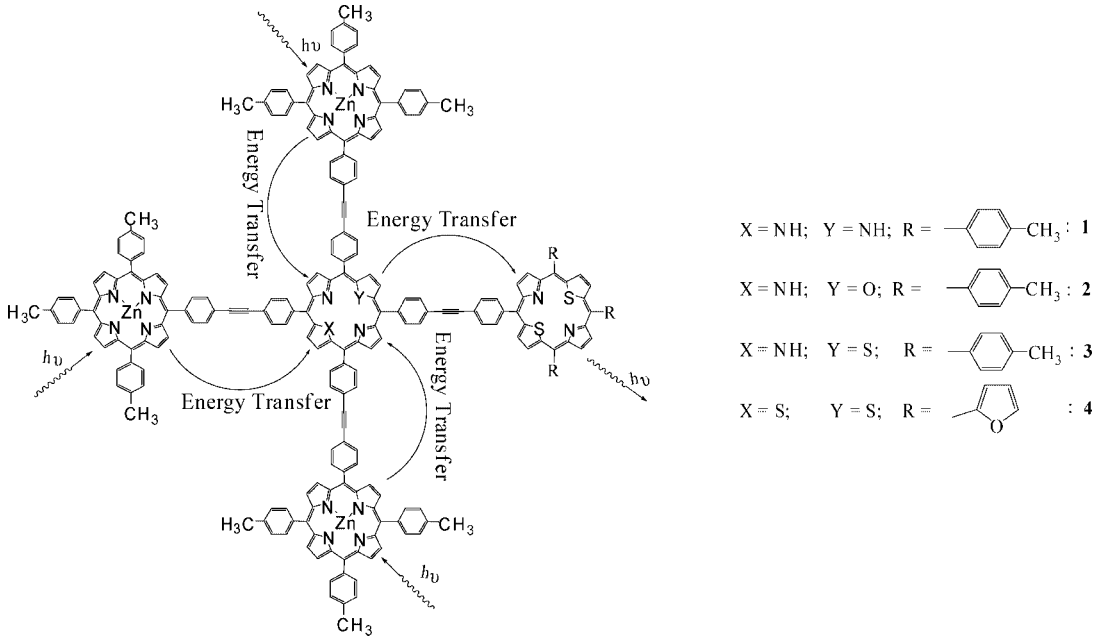

metrical diol[12c] methods to synthesize the monofunctionalized core-modified porphyrins and functionalized symmetrical diol method[14] to synthesize tetrafunctionalized A_4 type N_2S_2 porphyrin building blocks. The AB_3 type core-modified porphyrin building blocks were prepared by modifying the mono-ol and unsymmetrical diol methods.

The required precursors, the furan mono-ol, 2-{[4-(3-hydroxy-3-methylbut-1-ynyl)phenyl]hydroxymethyl}furan **9**, thiophene mono-ol, 2-{[4-(3-hydroxy-3-methylbut-1-ynyl)phenyl]hydroxymethyl}thiophene **10**, unsymmetrical thiophene diol, 2-[(4-iodophenyl) hydroxyl methyl]-5-{[4-(3-hydroxy-3-methyl but-1-ynyl) phenyl]-hydroxylmethyl} thiophene **11**, symmetrical thiophene diol, 2,5-bis[(4-iodo phenyl)hydroxymethyl]thiophene **12**, and symmetrical 16-thiatripyrrane, 5,10-di(4-iodophenyl)-16-thia-15,17-dihydrotripyrrane **13** were synthesized as shown in Scheme 1. The mono-ols **9** and **10** were synthesized[16] by treating furan and thiophene, respectively, with 1.2 equiv of *n*-BuLi followed by 1.2 equiv of 4-(3-hydroxy-3-methylbut-1-ynyl)benzaldehyde in THF at 0 °C. The crude compounds were subjected to column chromatographic purification and the pure mono-ols **9** and **10** were collected as white solids in 24% and 40% yields, respectively. The unsymmetrical diol **11** was synthesized similarly in 32% yield by treating mono-ol **10** with *n*-BuLi followed by 4-iodobenzaldehyde in THF at 0 °C and the resultant crude compound was purified by column chromatography on silica. The symmetrical thiophene diol **12** was synthesized in 65% yield by treating thiophene with 2.5 equiv of *n*-BuLi followed by treatment with 2.2 equiv of *p*-iodobenzaldehyde. The 16-thiatripyrrane **13** was synthesized[17] by reacting thiophene diol **12** with excess of pyrrole under mild acid-catalyzed conditions, and the crude compound was purified by silica gel column chromatography. The precursor compounds **9**−**13** were characterized by mp, IR, mass, NMR, and elemental analysis techniques.

The AB_3-type tetrafunctionalized N_3O and N_3S porphyrin building blocks **6** and **7**, respectively, were synthesized by condensing 1 equiv of mono-ol **9** and **10**, respectively, with 3 equiv of 4-iodobenzaldehyde and 3 equiv of pyrrole in propionic acid at refluxing temperature for 3 h (Scheme 1). The condensation resulted in the formation of mixture of two porphyrins: the desired AB_3-type tetrafunctionalized N_3O porphyrin **6** or N_3S porphyrin **7** and 5,10,15,20-tetrakis(4-iodophenyl)porphyrin with N_4 core. The mixture of two porphyrins was separated by column chromatography and afforded **6** and **7** in 6−7% yields. The AB_3-type tetrafunctionalized N_2S_2 porphyrin building block **8** was synthesized by condensing 1 equiv of diol **12** and 16-thiatripyrrane **13** in propionic acid at refluxing temperature for 2 h (Scheme 1). The condensation resulted in the formation of N_2S_2 porphyrin **8** as sole product. The crude compound was purified by column chromatography and afforded **8** as purple solid in 9% yield.

The tetrafunctionalized N_4, N_3O, N_3S, and N_2S_2 porphyrins **5**−**8** were characterized with ES-MS mass, NMR, absorption, fluorescence and elemental analysis techniques. All four tetrafunctionalized porphyrins **5**−**8** showed molecular ion peak in ES-MS mass spectra confirming the identity of the compounds (Supporting Information). In the ^{1}H NMR spectrum of **5**, the eight β-pyrrole protons appeared as singlet although multiplet is expected due to the unsymmetric substitution of N_4 porphyrin building block. Similarly, the N_3O porphyrin building block **6** showed a singlet for two β-furan protons and three sets of signals for six β-pyrrole protons. The N_3S porphyrin **7** showed a multiplet for two β-thiophene protons and three sets of signals for six β-pyrrole protons (Supporting Information). The four β-thiophene and four β-pyrrole protons in N_2S_2 porphyrin building block **8** appeared as two singlets. Thus, except N_3S porphyrin **7**, the other three porphyrins N_4 **5**, N_3O **6**, and N_2S_2 **8** porphyrins did not show the splitting of β-pyrrole, β-furan, and β-thiophene protons, although these porphyrins are unsymmetrically substituted. The absorption and emission spectra of N_4 **5**, N_3O **6**, N_3S **7**, and N_2S_2 **7** porphyrins showed characteristic porphyrin bands with peak maxima matching closely with corresponding symmetrically substituted *meso*-tetratolylporphyrins[11] such as H_2TTP, OTTPH, STTPH, and

(16) Ulman, A.; Manassen, J. *J. Chem. Soc., Perkin Trans.* **1979**, 1066.
(17) Heo, P.-Y.; Shin, K.; Lee, C.-H. *Bull. Korean Chem. Soc.* **1996**, *17*, 515.

SCHEME 1. Synthesis of AB_3-Type Tetrafunctionalized Porphyrins 6−8

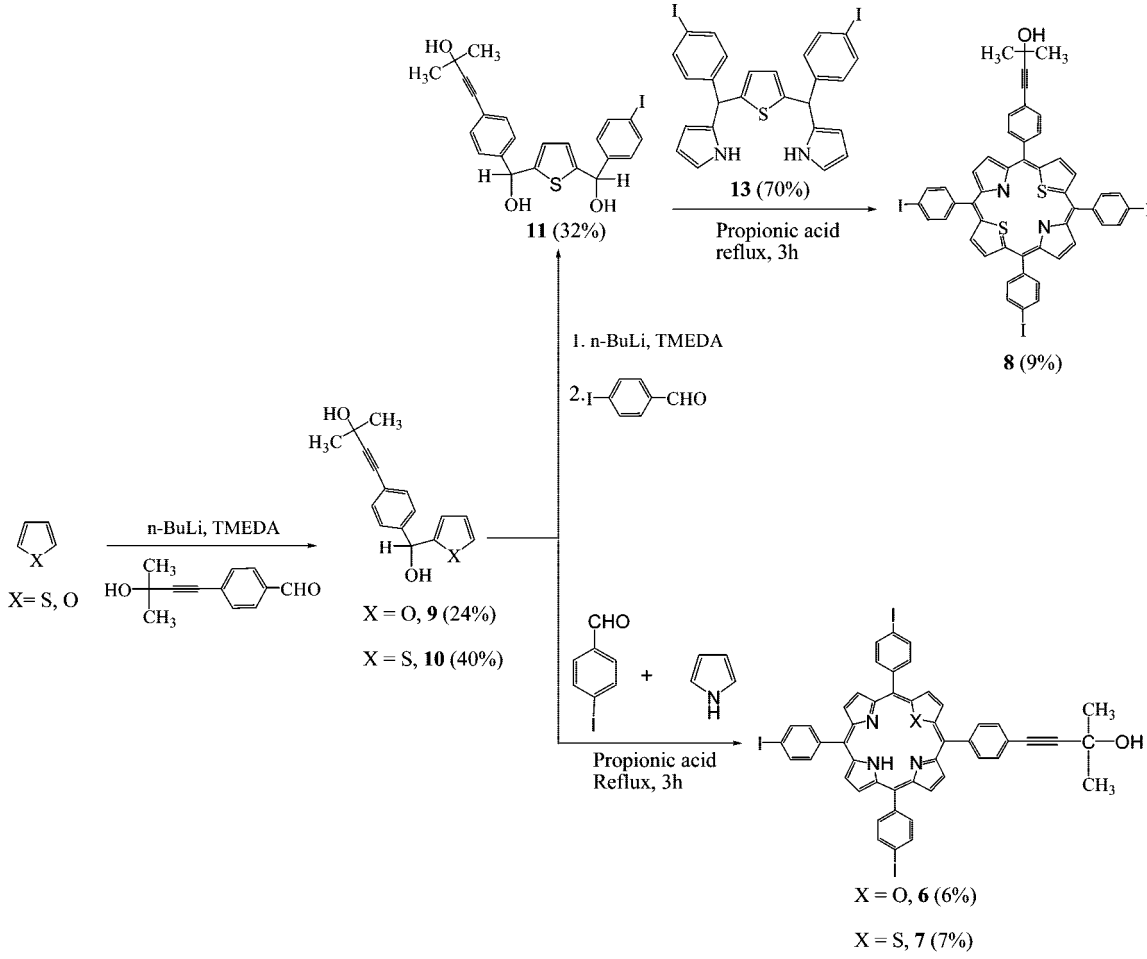

S_2TTP, respectively. The elemental analyses were also in agreement with the composition of the porphyrin building blocks **5**−**8**.

Synthesis of Covalently Linked Unsymmetrical Porphyrin Tetrads 14−17 and Pentads 1−4. The tetrafunctionalized porphyrin building blocks containing three *meso*-iodophenyl groups and one 3-hydroxy-3-methylbut-1-ynylphenyl group with different cores **5**−**8** were used to synthesize the monofunctionalized porphyrin tetrads containing two different macrocycles such as $(ZnN_4P)_3-N_4P$ **14**, $(ZnN_4P)-N_3OP$ **15**, $(ZnN_4P)_3-N_3SP$ **16**, and $(ZnN_4P)-N_2S_2P$ **17** as shown in Scheme 2. The other desired monofunctionalized porphyrin building block, 5-[4-(3-hydroxy-3-methylbut-1-ynyl)-10,15,20-tri(*p*-tolyl)zinc(II)porphyrin **18** was synthesized by following literature procedure.[18] The diphenylethyne bridged tetrads were synthesized under mild copper-free Pd(0) coupling conditions.[19] The tetrad **14** containing three ZnN_4 porphyrin subunits and one N_4 porphyrin subunit was synthesized by coupling of 3.2 equiv of **18** and 1 equiv of **5** in toluene/triethylamine at 40 °C in the presence of a catalytic amount of $AsPh_3$ and $Pd_2(dba)_3$ overnight. The TLC analysis after 12 h showed the appearance of new major spot along with two other minor spots corresponding to the starting materials. The crude compound was subjected twice to silica gel column chromatography and isolated pure tetrad **14** in 52% yield. Similarly, the tetrad $(ZnN_4P)_3-N_3OP$ **15** was prepared in 30% yield by coupling of **18** and **6** under similar Pd(0) coupling conditions. The tetrad $(ZnN_4P)_3-N_3SP$ **16** was obtained in 48% yield by coupling of **18** and **7** under similar reaction conditions. Coupling of **17** and **8** under the same mild Pd(0) conditions followed by silica gel column chromatographic purification afforded tetrad $(ZnN_4P)_3-N_2S_2P$ **17** in 50% yield. To afford the tetrads containing monoethynyl functional group **14a**−**17a**, the deprotection of ethynyl group of tetrads **14**−**17** was carried out by treating **14**−**17** with KOH in benzene/methanol at 80 °C (Scheme 2).

In the final step, the monofunctionalized tetrads **14a**−**17a** have been used to synthesize covalently linked unsymmetrical porphyrin pentads **1**−**4** containing three different porphyrin subunits (Scheme 3). The other required monofunctionalized N_2S_2 porphyrin building blocks such as 5-(4-iodophenyl)-10,15,20-tri(*p*-tolyl)-21,23-dithiaporphyrin[12c] **19** and 5-(4-iodophenyl)-10,15,20-tri(2-furyl)-21,23-dithiaporphyrin[12f] **20** were prepared as reported earlier. The $(ZnN_4)_3-N_4-N_2S_2$ porphyrin pentad **1** was synthesized by coupling of tetrad **14** and N_2S_2 porphyrin building block **19** in toluene/triethylamine at 35 °C in the presence of a catalytic amount of $AsPh_3/Pd_2(dba)_3$.[19] The progress of the reaction was monitored with TLC and the reaction was stopped after the disappearance of spots corresponding to starting materials and the appearance of new spot corresponding to unsymmetrical porphyrin pentad **1**. The crude

(18) Cho, W.-S.; Kim, H.-J.; Littler, B. J.; Miller, M. A.; Lee, C.-H.; Lindsey, J. S. *J. Org. Chem.* **1999**, *64*, 7890.

(19) (a) Wagner, R. W.; Johnson, T. E.; Li, F.; Lindsey, J. S. *J. Org. Chem.* **1995**, *60*, 5266–5273. (b) Farina, A.; Krishnan, V. B. *J. Am. Chem. Soc.* **1991**, *113*, 9585.

SCHEME 2. Synthesis of Covalently Linked Unsymmetrical $(ZnN_4)_3-N_3X$ Porphyrin Tetrads

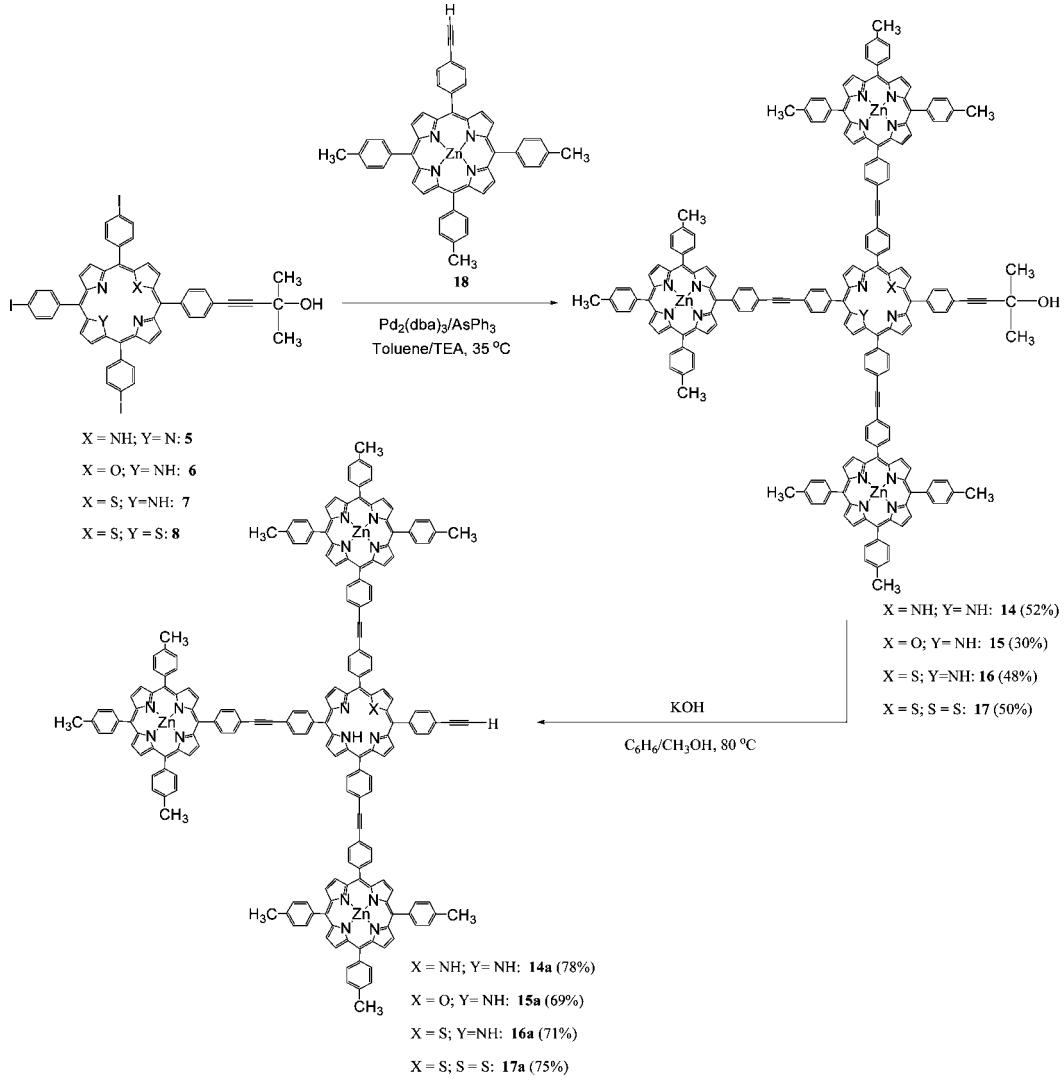

compound was subjected twice to silica gel column chromatography and afforded $(ZnN_4)_3-N_4-N_2S_2$ porphyrin pentad **1** in 52% yield. The pentads $(ZnN_4)_3-N_3O-N_2S_2$ **2** and $(ZnN_4)_3-N_3S-N_2S_2$ **3** were prepared by coupling of tetrads **15** and **16**, respectively, with N_2S_2 porphyrin building block **19** under similar mild Pd(0)-mediated coupling conditions.[19] The crude pentads **2** and **3** were purified by column chromatography and afforded pure compounds **2** and **3** in 30−40% yields. The pentad $(ZnN_4)-N_2S_2-N_2S_2$ **4** was prepared by coupling of tetrad **17** and N_2S_2 porphyrin building block **20** under same Pd(0) mediated coupling conditions[19] and afforded in 45% yield. All coupling reactions worked smoothly and the progress of the reaction was followed easily by tlc analysis at regular intervals. Two silica gel column chromatographic purifications are required to afford pure tetrads **14**−**17** and pentads **1**−**4** in decent yields and all compounds are readily soluble in most of the common organic solvents. The tetrads **14**−**17**, their deprotected forms **14a**−**17a**, and pentads **1**−**4** were characterized by ES-MS mass, NMR, elemental analysis, absorption, cyclic voltammetry, steady-state, and time-resolved fluorescence techniques. The tetrads **14**−**17**, deprotected tetrads **14a**−**17a**, and pentads **1**−**4** showed molecular ion peak in ES-MS mass spectra confirming the identity of the compounds (Supporting Information).

NMR Studies of Tetrads 14−17, and Pentads 1−4. NMR spectroscopy was used to characterize the tetrads **14**−**17** deprotected tetrads **14a**−**17a** and pentads **1**−**4** in detail. Since tetrads **14**−**17** and pentads **1**−**4** have two and three different types of porphyrin subunits respectively, the ^{1}H NMR resonances of tetrads and pentads were assigned on the basis of spectra observed for the two and three constituted porphyrin monomers of corresponding tetrad and pentad taken independently.

In the ^{1}H NMR spectrum of tetrad **14** containing three ZnN_4 porphyrin subunits and one N_4 porphyrin subunits, the 32 β-pyrrole protons; 24 protons corresponding to three ZnN_4 porphyrin subunits and 8 protons corresponding to N_4 porphyrin subunit were appeared as overlapping signals in 8.60−9.10 ppm region. The two inner NH protons of N_4 porphyrin subunit appeared at −2.80 ppm. In tetrad **15** containing three ZnN_4 porphyrin subunits and one N_3O porphyrin subunit, although the 30 pyrrole signals were appeared as series of overlapping signals in 8.80−9.00 ppm region, the two β-furan protons were appeared separately as multiplet in 9.16−9.18 ppm region confirming the composition of the tetrad. Similarly in the ^{1}H NMR spectrum of tetrad **16** containing one N_3S porphyrin and three ZnN_4 porphyrin subunits, the two β-thiophene protons of N_3S porphyrin subunit were observed as two sets of doublets in 9.60−9.80 ppm region and the β-pyrrole protons of all four

SCHEME 3. Synthesis of Covalently Linked Unsymmetrical $(ZnN_4)_3-N_2XY-N_2S_2$ Porphyrin Pentads 1−4

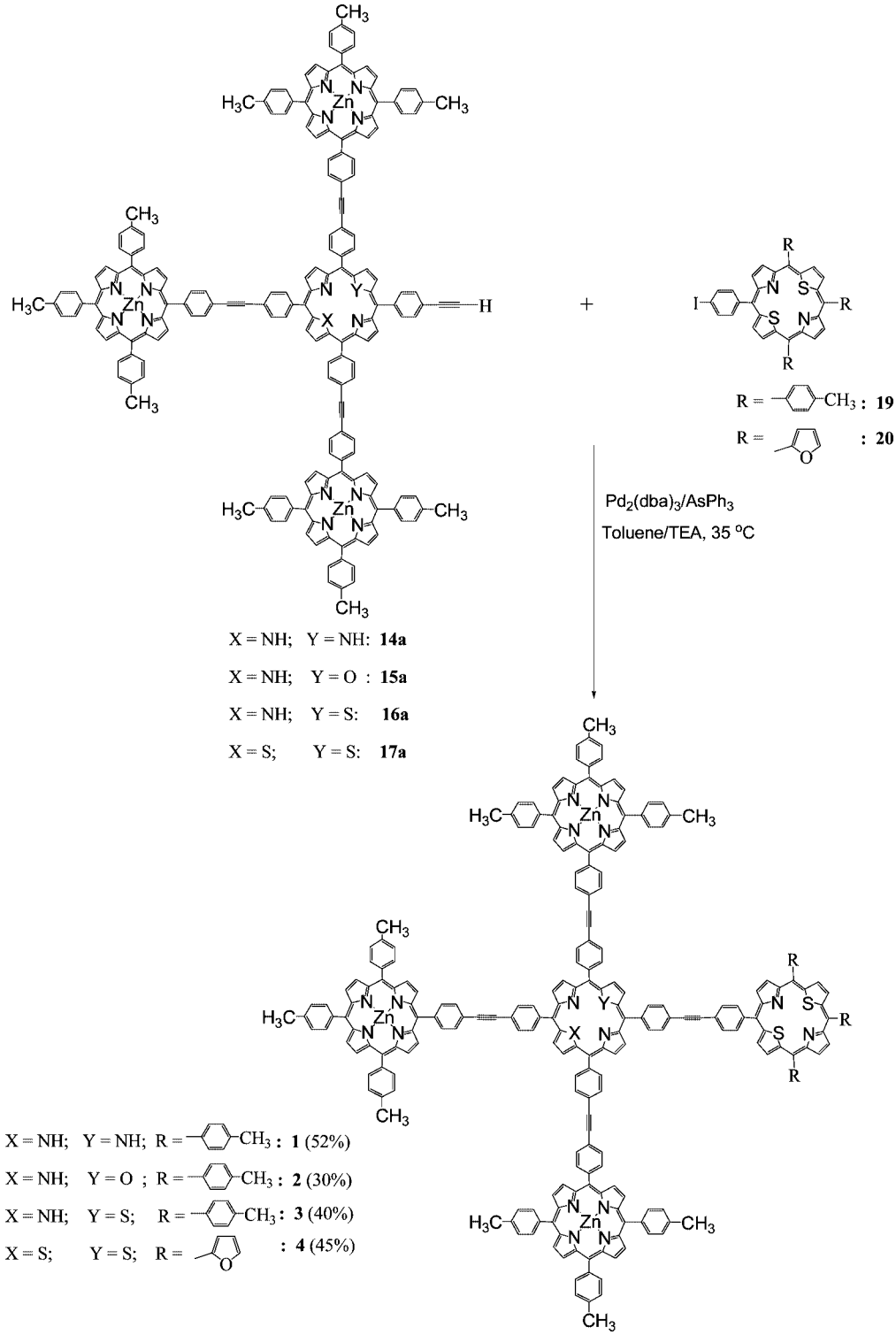

porphyrin subunits were appeared as overlapping signals in 8.60−9.00 ppm region. The tetrad **17** containing one N_2S_2 porphyrin and three ZnN_4 porphyrin subunits also showed two sets of doublets for four β-thiophene protons of N_2S_2 porphyrin subunit in 9.60−9.80 ppm as expected. The ^{1}H NMR spectra of deprotected tetrads **14a−17a** also exhibited same features as described for tetrads **14−17**. The signal at $\delta = 3.3$ ppm corresponding to ethyne CH proton in ^{1}H NMR spectra confirmed the identity of the porphyrin tetrads **14a−17a** containing one phenylethynyl functional group.

The pentads **1−4** containing three different porphyrin subunits showed resonances corresponding to all three porphyrin subunits in ^{1}H NMR spectra (Supporting Information). For, e.g., pentad **2** containing ZnN_4, N_3O, and N_2S_2 porphyrin subunits, the specific resonances corresponding to each porphyrin subunit such as signals at 9.2 ppm of β-furan protons of N_3O porphyrin subunit and signals at 9.8 ppm of β-thiophene protons of N_2S_2 porphyrin subunit were present (Supporting Information). Similarly, the other three pentads **1**, **3**, and **4** also showed features corresponding to three different porphyrin subunits. A

TABLE 1. Absorption Data of Porphyrin Tetrads 14−17 and a 3:1 Mixture of Corresponding Monomers Recorded in Toluene

porphyrin	Soret band λ (nm) ($\epsilon \times 10^{-4}$)	absorption Q-bands λ (nm) ($\epsilon \times 10^{-3}$)
14	420 (45.2)	516 (22.2), 551 (9.5), 593 (6.4), 649 (5.5)
3:1 mixture of **18** and **5**	419 (101.1)	515 (29.2), 550 (48.9), 590 (14.4), 650 (15.6)
15	423 (45.2)	515 (21.2), 552 (9.2), 592 (8.4), 619 (6.4), 673 (5.5)
3:1 mixture of **18** and **6**	422 (90.2)	515 (27.3), 550 (42.9), 593 (16.1), 618 (15.2), 672 (12.2)
16	423 (sh) 430 (18.6)	516 (15.5), 550 (5.4), 592 (4.2), 624 (2.4) 679 (3.8)
3:1 mixture of **18** and **7**	420 (89.2)	515 (26.2), 550 (38.7), 592 (15.9), 625 (14.8), 678 (9.2)
17	422 (21.3) 435 (sh)	514 (19.3), 552 (5.8), 592 (1.4), 631 (3.5) 699 (3.6)
3:1 mixture of **18** and **8**	420 (88.7)	515 (27.2), 552 (38.9), 592 (16.2), 631 (14.8), 699 (9.9)

TABLE 2. Absorption Data of Porphyrin Pentads 1−4 and 1:1 Mixture of Their Corresponding Tetrads and Monomers Recorded in Toluene

compd	Soret band λ (nm) ($\epsilon \times 10^{-4}$)	absorption Q-bands λ (nm) ($\epsilon \times 10^{-3}$)
1	420 (40.2) 436 (36.4)	516 (22.2), 551 (9.5), 593 (6.2), 649 (5.1), 699 (3.2)
1:1 mixture of **14** and **19**	420 (99.2) 436 (89.5)	515 (42.6), 550 (16.8), 592 (13.9), 650 (20.2) 698 (10.1)
2	424 (31.8) 436 (20.8)	516 (20.2), 551 (8.9), 590 (6.2), 616 (5.8) 672 (4.2), 699 (sh)
1:1 mixture of **15** and **19**	421 (97.2) 436 (sh)	515 (46.5), 550 (16.6), 590 (13.9), 616 (19.2) 672 (10.6), 699 (7.4)
3	423 (23.9) 436 (20.2)	515 (17.5), 552 (11.2), 590 (5.4), 635 (4.4), 680 (sh), 699 (3.2)
1:1 mixture of **16** and **19**	432 (92.5) 436 (sh)	516 (45.8), 551 (22.3), 590 (15.6), 636 (18.6) 679 (4.5), 699 (7.2)
4	422 (25.4) 454 (sh)	517 (17.8), 551 (12.4), 573 (5.6), 590 (5.3), 702 (3.8), 717 (sh)
1:1 mixture of **17** and **20**	422 (93.9) 452 (sh)	515 (46.9), 551 (25.6), 573 (16.2), 590 (19.2) 700 (10.1), 717 (6.8)

comparison of chemical shifts of the various protons of tetrads **14**−**17** and pentads **1**−**4** with those of corresponding monomeric porphyrin units indicate only minor differences, suggesting that the porphyrin subunits in tetrads **14**−**17** and pentads **1**−**4** interact very weakly.

Absorption Properties of Tetrads 14−17 and Pentads 1−4. The absorption spectra of tetrads **14**−**17** and their corresponding porphyrin monomers in 3:1 ratio and pentads **1**−**4** and their corresponding 1:1 mixture of tetrad and N_2S_2 porphyrin monomers were recorded in toluene and data are presented in Tables 1 and 2, respectively. The comparison of absorption spectra of tetrad **17** and 3:1 mixture of monomers of ZnN_4 porphyrin and N_2S_2 porphyrin recorded in toluene is shown in Figure 1. Inspection of Figure 1 and Table 1 indicates that the absorption spectra of tetrads showed features of both monomeric porphyrin subunits[11] with almost no shifts in peak maxima indicating that the constituted monomeric porphyrins retained their properties in tetrads. For example, in tetrad **17**, the absorption bands at 699, 631, and 514 nm in the Q-band region mainly correspond to N_2S_2 porphyrin subunit and the bands at 552 and 592 nm belong to the ZnN_4 porphyrin subunit. Similarly, the Soret band at 435 nm corresponds to the N_2S_2 porphyrin subunit and the band at 422 nm appeared as shoulder corresponds to ZnN_4 porphyrin subunits. The other three tetrads **14**−**16** also showed similar absorption features. The Soret band in tetrads **14**−**16** did not show any splitting but broadened because the peak maxima of the corresponding monomers of the tetrads **14**−**16** were close to each other. However, the extinction coefficients of all absorption bands of tetrads **14**−**17** compared to their 3:1 mixture of corresponding monomers (Table 1) were quite different, indicating that the porphyrin subunits in tetrads **14**−**17** interact very weakly.

The comparison of absorption spectra of $(ZnN_4)_3-N_3S$ tetrad **16** and (ZnN_4)−-$N_3S-N_2S_2$ pentad **3** is shown in Figure 2. The absorption spectra of pentad **1**−**4** are just linear combination of the spectra of all three different macrocycles with only minor differences in wavelength maxima and band shapes. For example, the (ZnN4)−-$N_3S-N_2S_2$ pentad **3** (Figure 2) showed six absorption bands in the Q-band region with absorption maxima at 515, 552, 590, 635, 680, and 699 nm and two bands in the Soret region with peak maxima at 423 and 436 nm (Table 2). In this pentad **3**, the absorption bands at 699, 635, and 436 nm mainly correspond to N_2S_2 porphyrin subunit; 680 nm is exclusively from the N_3S porphyrin subunit, and bands at 590, 550, and 423 nm are mainly because of the ZnN_4 porphyrin subunit. Unlike tetrads **14**−**17** which showed a broad Soret band, the pentads **1**−**4** showed a split Soret band. This is due to the relatively large difference between the Soret absorption peak maxima of the three different macrocycles of the pentad. Similarly, the absorption spectra of the other three pentads **1**, **2**, and **4** are nearly the sum of the spectra of the corresponding three different macrocycles of those pentads (Table 2). Although the peak maxima of absorption bands of pentads is nearly same as those of their corresponding monomers, the extinction coefficients of pentads are much lower than 1:1 mixture of their corresponding tetrad and N_2S_2 porphyrin monomer (Table 2) indicating that the porphyrin subunits in the pentad interact very weakly.

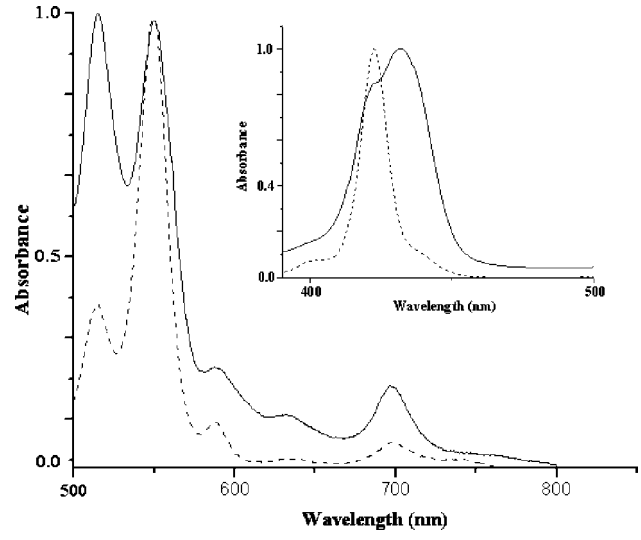

FIGURE 1. Comparison of Q-band and Soret band (inset) absorption spectra of $(ZnN_4P)_3-N_2S_2P$ tetrad **17** (—) and 3:1 mixture of corresponding monomers (---) recorded in toluene.

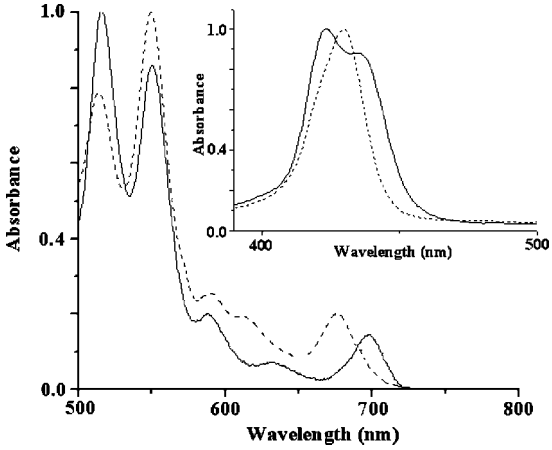

FIGURE 2. Q-band absorption spectra of **3** (—) and **16** (---) recorded in toluene. The inset shows their corresponding Soret band absorption spectra. The concentrations used for Q- and Soret band spectra were 5 × 10^{-5} M and 5 × 10^{-6} M, respectively.

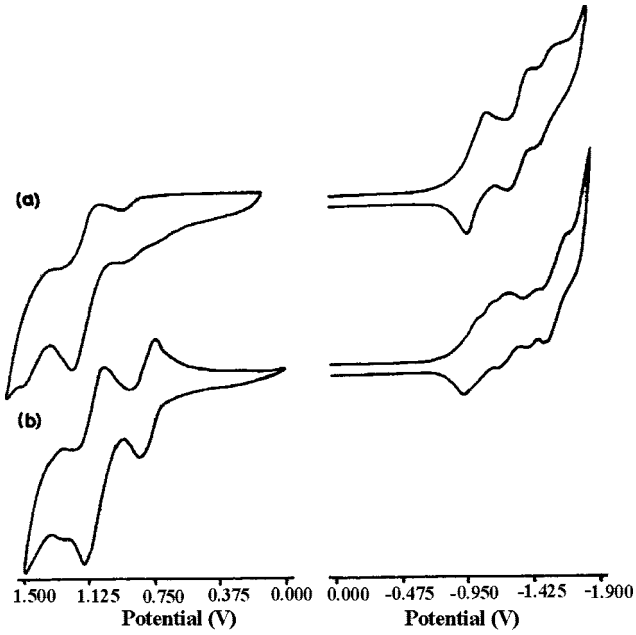

FIGURE 3. Comparison of cyclic voltammograms (scan rate, 50 mVs^{-1}) of (a) tetrad **16** and (b) pentad **3** in CH_2Cl_2 containing 0.1 M TBAP as supporting electrolyte.

Electrochemical Properties of Tetrads 14−17. The redox chemistry of covalently linked unsymmetrical porphyrin tetrads **14−17** containing two different macrocycles and porphyrin pentads **1−4** containing three different macrocycles was followed by cyclic voltammetry at a scan rate of 50 mV/s and differential pulse voltammetry at a scan rate of 20 mV/s using tetrabutylammonium perchlorate as supporting electrolyte (0.1 M) in dichloromethane. In general, the oxidation and reduction waves of two porphyrin subunits in tetrads **14−17** and three porphyrin subunits in pentads **1−4** were present and the peak potentials were matching closely with the corresponding monomeric porphyrins. The tetrads **14−17** showed three oxidations and three reductions (Figure 3). Both oxidations and reductions are reversible or quasi-reversible (E_p = 60−120 mV), and all potentials were assigned easily on the basis of electrochemical data of their corresponding monomers[11] (Table 3). For example, the tetrad **14** showed three oxidations at 0.73, 0.98, and 1.28 V. The first oxidation

TABLE 3. Electrochemical Redox Data (V) of Porphyrin Monomers, Tetrads 14−17, and Pentads 1−4 in Dichloromethane Containing 0.1 M TBAP as Supporting Electrolyte

compd	oxidation				reduction			E_{CT} (M^+, M^-)	E_{0-0}
18	0.77	1.08			−1.35		−1.71		2.06
5		1.03	1.30	−1.11		−1.52			1.90
6		1.10			−1.20				1.85
7		1.11	1.28	−1.03	−1.35				1.82
8		1.18		−0.94	−1.23				1.77
20		0.92	1.24	−0.82	−1.18				1.63
14	0.73	0.98	1.28		−1.18	−1.55	−1.75	1.91	
15	0.72	0.92	1.23		−1.16	−1.54	−1.75	1.88	
16	0.72	1.02	1.39	−1.02		−1.46	−1.69	1.74	
17	0.71	1.01	1.38	−0.98	−1.22		−1.72	1.61	
1	0.72	1.03	1.31	−0.93	−1.18	−1.53	−1.75	1.62	
2	0.72	0.91	1.24	−0.90	−1.29	−1.51	−1.74	1.62	
3	0.70	1.02	1.29	−0.92	−1.10 −1.22	−1.40	−1.64	1.62	
4	0.72	0.98	1.25	−0.80	−1.03 −1.27	−1.56	−1.73	1.52	

at 0.73 V was due to oxidation of the ZnN_4P subunit because it is easier to oxidize as compared to free base N_4P. The oxidation at 1.28 V was assigned to the oxidation of N_4P, and oxidation at 0.98 V was due to the oxidation of both ZnN_4P and N_4P subunits. Similarly, the three reductions of **14** at −1.18, −1.55, and −1.75 V were assigned as follows: the first reduction at −1.18 V was due to N_4P porphyrin, the last reduction at −1.75 V was assigned to ZnN_4P porphyrin, and reduction at −1.55 V was due to to both N_4P and ZnN_4P porphyrin subunits. Similarly, the tetrads **15−17** also exhibited oxidation and reduction waves, and the peak potentials were in the same range of their corresponding porphyrin monomers (Table 3). Pentads **1−4** also exhibited similar redox features. Although all three different porphyrin subunits of pentads **1−4** have one or two overlapping redox potentials, it is noted that atleast one oxidation or reduction wave which is an exclusive characteristic feature of each porphyrin subunit of the pentad is present. For example, in ZnN_4 porphyrin, $(ZnN_4)_3$−N_3S porphyrin tetrad **16** and $(ZnN_4)_3$−N_3S−N_2S_2 porphyrin pentad **3** series, the ZnN_4 porphyrin shows a specific oxidation at 0.71 V, the $(ZnN_4)_3$−N_3S porphyrin tetrad **16** showed a specific reduction at −1.02 V corresponding to N_3S porphyrin subunit and $(ZnN_4)_3$−N_3S−N_2S_2 porphyrin pentad **3** showed a specific reduction at −0.92 V characteristic of the N_2S_2 porphyrin subunit of pentad **3**. These specific oxidation and reduction potentials help in the characterization of these compounds. Thus, the electrochemical studies were in agreement with the absorption studies of tetrads **14−17** and pentads **1−4** and studies support that the porphyrin subunits in tetrads and pentads interact very weakly.

Steady-State and Time-Resolved Fluorescence Studies of Tetrads 14−17 and Pentads 1−4. The steady-state fluorescence properties of tetrads **14−17**, pentads **1−4**, and appropriate reference compounds were recorded in toluene at room temperature (Table 4). In tetrads **14−17**, the ZnN_4 porphyrin subunit acts as an energy donor and absorbs strongly at 550 nm, and N_4, N_3O, N_3S, and N_2S_2 porphyrin subunits act as energy acceptors and do not absorb strongly at 550 nm. The emission spectra of tetrad **17** along with its 3:1 mixture of ZnN_4 and N_2S_2 porphyrins using excitation wavelength of 550 nm and an excitation spectrum of tetrad **17** using emission wavelength of 750 nm recorded in toluene are shown in Figure 4. Inspection of Figure 4 indicates that on illumination of tetrad **17** at 550 nm where the ZnN_4 porphyrin subunit absorbs strongly, the emission of ZnN_4 causes the porphyrin subunit to

TABLE 4. Emission Data of Tetrads 14−17 and Pentads 1−4 in Toluene

compd	Φ_f (donor)	% donor	τ_{DA} (ps)	Φ_{ENT}	K_{ENT}^{-1} (ps)
ZnTPP	0.033		2070		
14	0.0006	98	66	0.97	68
15	0.0008	98	89	0.95	93
16	0.0010	97	99	0.95	104
17	0.0006	98	136	0.94	145
1	0.0007	98	80	0.96	83
2	0.0008	98	112	0.94	118
3	0.0012	96	128	0.94	136
4	0.0010	97	142	0.93	152

be quenched by 98%, and the strong emission was observed from N_2S_2 porphyrin subunit. However, when a 3:1 mixture of ZnN_4 porphyrin and N_2S_2 porphyrin was excited at 550 nm, the strong emission was exclusively observed from ZnN_4 porphyrin. The excitation spectrum of tetrad **17** recorded at 750 nm matched with the absorption spectrum. These results indicated that there is an efficient singlet−singlet energy transfer from ZnN_4 porphyrin subunit to N_2S_2 porphyrin subunit in tetrad **17**. Similarly, for the tetrads **14**−**16** on excitation at 550 nm, the emission from ZnN_4 porphyrin was quenched by 97−98% and the strong emission was observed from N_4, N_3O, and N_3S porphyrin subunits, respectively, supporting an efficient energy transfer from the ZnN_4 porphyrin subunit to the respective acceptor porphyrin subunit in tetrads **14**−**16**.

The emission spectra of pentad **3** and a 3:1:1 mixture of the corresponding monomers recorded at 550 nm is shown in Figure 5. As is evident from Figure 5, in the pentad **3**, excitation at 550 nm, where the ZnN_4 porphyrin subunit absorbs strongly (ϕ = 0.033 for ZnTPP), the emission of the ZnN_4 porphyrin subunit was quenched by 97% (ϕ = 0.0008) and the strong emission from the N_2S_2 porphyrin subunit was observed. However, when a 3:1:1 mixture of corresponding monomers was irradiated at 550 nm, a strong emission was observed mainly from the ZnN_4 porphyrin subunit (Figure 5). These results indicate that there is an efficient energy transfer from the ZnN_4 porphyrin subunit to the N_2S_2 porphyrin subunit in pentad **3**. The energy transfer that occurs in **3** is independent of the excitation wavelength. The excitation spectrum recorded for **3** at λ_{em} = 730 nm matches with the absorption spectrum, further confirming the efficient energy transfer among the subunits.

The tetrads **14**−**17**and pentads **1**−**4** were studied by time-resolved fluorescence spectroscopic technique which also support the efficient energy transfer within tetrads **14**−**17** and pentads **1**−**4**. The tetrads **14**−**17** were excited at 406 nm and monitored at two different wavelengths corresponding to the emission peak maxima of donor ZnN_4 porphyrin subunit and acceptor porphyrin such as N_4 in **14**, N_3O in **15**, N_3S in **16**, and N_2S_2 in **17**. The fluorescence decays of tetrads **14**−**17** monitored at emission peak maxima of acceptor porphyrin subunit was fitted to single exponential and the lifetime was close to the corresponding porphyrin monomer. The fluorescence decays of tetrads **14**−**17** monitored at emission peak maxima of donor ZnN_4 porphyrin subunit were fitted to two or three exponential with a dominant contribution from one component (Supporting Information). The other one or two minor components observed were attributed to the monomeric porphyrin impurities present in the tetrad. The major component decay is generally the

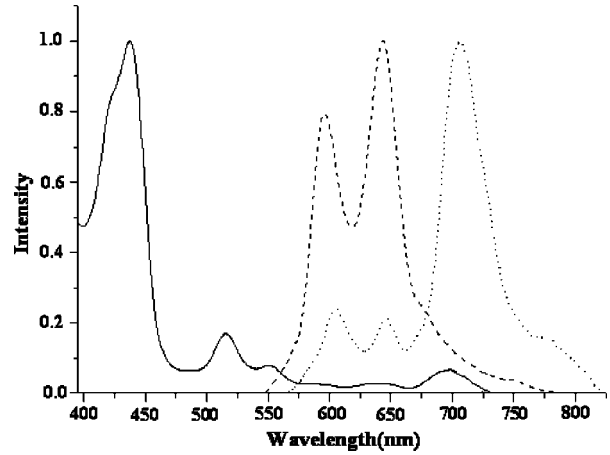

FIGURE 4. Comparison of emission spectra of $(ZnN_4P)_3-N_2S_2P$ tetrad **17** (···), and 3:1 mixture of **8** and **18** (---) recorded at an excitation wavelength 550 nm in toluene. The excitation spectrum of tetrad **17** (—) recorded at emission wavelength 750 nm is also shown.

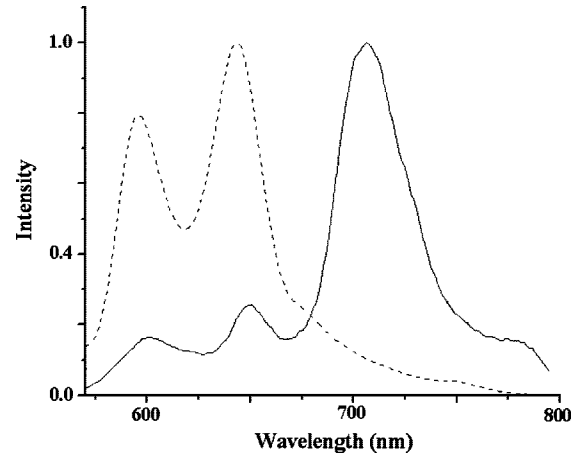

FIGURE 5. Comparison of emission spectra of pentad **3** (—) and 3:1:1 mixture of corresponding monomers (---) recorded at excitation wavelength 550 nm in toluene.

quenched lifetime of donor ZnN_4 porphyrin subunit. The donor ZnN_4porphyrin subunit was quenched due to singlet−singlet energy transfer from donor ZnN_4 porphyrin subunit to the acceptor porphyrin subunit in tetrad such as N_4 in **14**, N_3O in **15**, N_3S in **16**, and N_2S_2 porphyrin subunit in **17**. The rate of energy transfer (k_{ENT}) and the efficiency of energy transfer (ϕ_{ENT}) were calculated[20] from the measured lifetime (τ_{DA}) of the ZnN_4 porphyrin subunit in tetrads and ZnTPP (τ_D) using the following equations:

$$k_{ENT} = 1/\tau_{DA} - 1/\tau_D \quad (1)$$

$$\varphi_{ENT} = k_{ENT}\tau_D \quad (2)$$

The k_{ENT} and ϕ_{ENT} data indicate that the efficiencies (>90%) are almost same as that of diphenylethyne bridged porphyrin dyads reported in literature[21] but the energy transfer rates are found to be slower than the reported dyads.[2a,b,20] Furthermore, we evaluated through-bond (TB) and through-space (TS) contributions to the overall rate of energy transfer in terms of Förster theory.[21] The Förster process is mediated by the donor−acceptor distance and orientation as well as their

(20) Hsiao, J.-S. B. P; Krueger, B. P.; Wagner, R. W.; Johnson, T. E.; Delaney, J. K.; Mauzerall, D. C.; Fleming, G. R.; Lindsey, J. S.; Bocian, D. F.; Donohoe, R. J. *J. Am. Chem. Soc.* **1996**, *118*, 11181.

(21) Förster, Th. *Ann. Phys.* **1948**, *2*, 55.

TABLE 5. Through-Bond and through-Space Energy Transfer Rates and Contributions for Covalently Linked Porphyrin Tetrads 14−17 and Pentads 1−4

compd	J (10^{-14})	K_{TS}^{-1} (ps)	K_{TB}^{-1} (ps)	χ_{TS}	χ_{TB}
14	4.22	473	79	0.14	0.86
15	4.05	498	116	0.19	0.81
16	1.91	1040	116	0.10	0.90
17	4.31	763	178	0.18	0.82
1	4.48	617	99	0.13	0.86
2	4.52	1612	127	0.07	0.92
3	4.97	546	181	0.24	0.75
4	7.98	719	193	0.20	0.80

emission and absorption spectral overlap characteristics. In the Förster theory of energy transfer, the rate is given by

$$k_{TS} = (8.8 \times 10^{23}) K^2 \varphi_f J n^{-4} \tau_D^{-1} R^{-6} \quad (3)$$

where K^2 is the orientation factor, ϕ_f is the fluorescence quantum yield of the donor in the absence of acceptor, J (in cm^6 mmol^{-1}) is the spectral overlap integral, n is the solvent refractive index (1.49 for toluene), τ_D is the donor lifetime in the absence of acceptor and R is the center-to-center distance of donor−acceptor in Å. The overlap integral J is calculated from the equation

$$J = F_D(\nu)\varepsilon(\nu)\nu^{-1}d\nu \quad (4)$$

where F_D (ν) is the fluorescence intensity of the donor in wavenumber units with total intensity normalized to unity, $\epsilon(\nu)$ is the absorbance coefficient of the acceptor and ν is the wavenumber in cm^{-1}. The center-to-center distance of donor−acceptor was taken as 20 Å based on MM$^+$ force field calculations, and 1.125 was used for K^2. The relative contributions of TS (χ_{TS}) and TB (χ_{TB}) energy transfer to overall rate were calculated using the following equations:[20]

$$k_{ENT} = k_{TB} + k_{TS} \quad (5)$$

$$\chi_{TS} = k_{TS}/k_{ENT} \quad (6)$$

$$\chi_{TB} = k_{TB}/k_{ENT} \quad (7)$$

The data presented in Table 5 reveals that the TB contribution accounts for greater than 90% of the observed rate as noted previously for similar kind of diarylethyne bridged porphyrin arrays.[2a,b,20] In addition to energy transfer, the electron-transfer quenching interaction may also be possible in these systems. Hence we evaluated the single state energy levels and charge transfer states using fluorescence and redox potential data[22] (Figure 6). As shown in Figure 6, the quenching of ZnN_4 porphyrin fluorescence is also partly due to the photoinduced electron transfer which is also possible in these tetrads.

The time-resolved emission studies also support the efficient energy transfer in pentads **1**−**4**. The fluorescence decays of pentads were fitted to two or three exponential with one major component (95%) and one or two minor components. The minor components are due to small impurities of monomeric porphyrins present in the pentads. The major component decay was attributed to the decreased lifetime of ZnN_4 porphyrin subunit in pentads due to the singlet−singlet excitation energy transfer from the ZnN_4 porphyrin subunit to the terminal N_2S_2 porphyrin subunit. The K_{ENT} and ϕ_{ENT} calculated for pentads **1**−**4** indicate that the efficiencies (90%) are good, but the energy transfer rates are slower than the reported porphyrin arrays. Furthermore, it is established that in pentads also through-bond contribution accounts for greater than 90% of the observed rate (Table 5). The energy level diagram shown in Figure 6 suggest that the photoinduced electron transfer was also partly responsible in addition to energy transfer for quenching of ZnN_4 porphyrin emission in pentads **1**−**4**. A detailed photophysical studies are required to understand the excited-state dynamics of porphyrin pentads with three different porphyrin subunits reported in this paper.

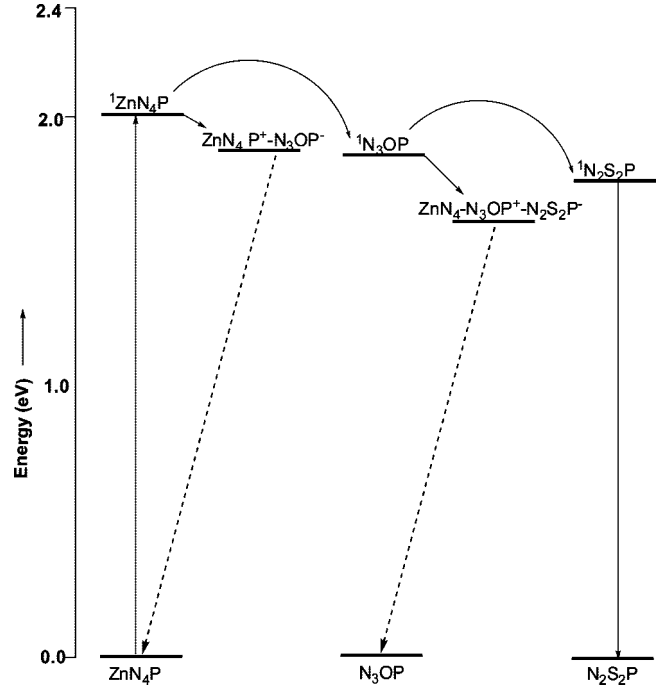

FIGURE 6. Energies of singlet and charge-transfer states of the pentad **2** containing ZnN_4, N_3O, and N_2S_2 porphyrin subunits.

Conclusions

In conclusion, we synthesized four new AB_3-type tetrafunctionalized porphyrin monomeric building blocks with N_4, N_3O, N_3S, and N_2S_2 cores by modifying the existing methods. The tetrafunctionalized porphyrin building blocks were used to synthesize the monofunctionalized porphyrin tetrads by coupling of one equivalent of AB_3 type tetrafunctionalized porphyrin building block with 3 equiv of monofunctionalized ZnN_4 porphyrin building blocks under Pd(0) coupling conditions. In the final step, the monofunctionalized porphyrin tetrads were coupled with monofunctionalized N_2S_2 porphyrin building blocks under similar Pd(0) coupling conditions and afforded porphyrin pentads containing three different porphyrin cores in decent yields. The unsymmetrical porphyrin tetrads containing two different porphyrin cores and unsymmetrical porphyrin pentads containing three different porphyrin cores were characterized by spectral and electrochemical techniques. The NMR, absorption, and electrochemical studies on unsymmetrical porphyrin tetrads and pentads indicate that the two and three types of porphyrin subunits in tetrads and pentads respectively retain their individual properties supporting weak interaction among the porphyrin subunits. The steady state and time-resolved fluorescence studies support an efficient energy transfer at singlet state from peripheral donor ZnN_4 porphyrin subunits to N_4, N_3S, N_3O, and N_2S_2 porphyrin subunits in tetrads and peripheral ZnN_4 porphyrin subunits to acceptor N_2S_2 porphyrin subunit mediated via central N_4, N_3O, N_3S, and N_2S_2 porphyrin

(22) Giribabu, L.; Rao, T. A.; Maiya, B. G. *Inorg. Chem.* **1999**, *38*, 4971.

subunits in pentads. More studies are required to understand the excited-state dynamics of these novel pentads containing three different cores. The synthetic strategy shown in this paper would help in designing and synthesizing more elaborate novel unsymmetrical porphyrin arrays containing different porphyrin subunits.

Experimental Section

$(ZnN_4)_3-N_4-N_2S_2$ Porphyrin Pentad (1). Samples of tetrad **14a** (10.0 mg, 3.49 μmol) and 5-(4-iodophenyl)-10,15,20-tri(*p*-tolyl)-21,23-dithiaporphyrin **20** (2.85 mg, 3.49 μmol) in dry toluene/triethylamine (3:1, 20 mL) were coupled in the presence of catalytic amounts of $AsPh_3$ (1.28 mg, 4.18 μmol) and $Pd_2(dba)_3$ (0.48 mg, 0.52 μmol) at 35 °C for 15 h. The formation of pentad was confirmed by the appearance of new spot on TLC as well as the characteristic absorption bands observed in UV−vis spectroscopy. The crude compound was purified by silica gel column chromatography, and the pure porphyrin pentad **1** was collected using dichloromethane/methanol (93:7) as a purple solid (6 mg, 52%). Mp > 300 °C. IR (KBr film): ν = 3356, 3058, 2930, 2875, 2110, 1451, 990, 853, 752 cm^{-1}. ^{1}H NMR (400 MHz, $CDCl_3$, 25 °C): δ = −2.84 (s, 2H), 2.72 (s, 36H), 7.42−7.49 (m, 30H), 7.80 (d, J = 8.0 Hz, 10H), 8.09−8.12 (m, 40H), 8.78−8.90 (m, 36H), 9.59−9.64 (m, 4H) ppm. ^{13}C NMR (100 MHz, $CDCl_3$, 25 °C): 22.4, 90.9, 93.8, 124.5, 126.2, 126.1, 127.6, 128.9, 130.1, 130.9, 132.6, 133.6, 134.5, 134.9, 135.6, 137.2, 140.4, 142.8, 142.7, 143.4, 145.2, 147.2, 147.9, 149.1, 150.4, 151.6, 153.8 ppm. Anal. Calcd: C, 81.10; H, 4.48; N, 7.09; S, 1.80. Found: C, 81.32; H, 4.62; N, 7.20; S, 1.64.

$(ZnN_4)_3-N_3O-N_2S_2$ Porphyrin Pentad 2. Samples of porphyrin tetrad **15a** (10.0 mg, 3.49 μmol) and 5-(4-iodophenyl)-10,15,20-tri(*p*-tolyl)-21,23-dithiaporphyrin **20** (2.85 mg, 3.49 μmol) in dry toluene/triethylamine (3:1, 30 mL) were coupled in the presence of $AsPh_3$ (1.28 mg, 4.18 μmol) and $Pd_2(dba)_3$ (0.48 mg, 0.52 μmol) at 35 °C for 12 h. The crude reaction mixture was purified by silica gel chromatography using dichloromethane /methanol (90:10) and afforded pentad **2** as a purple solid in 30% yield (4 mg). Mp > 300 °C. IR (KBr film): ν = 3348, 3055, 2923, 2854, 1452, 995, 750 cm^{-1}. ^{1}H NMR (400 MHz, $CDCl_3$, 25 °C): δ = 2.75 (s, 36H), 7.30−7.38 (m, 36H), 7.50−7.64 (m, 12H), 7.88−8.00 (m, 10H), 8.05−8.18 (m, 22H), 8.62−8.70 (m, 20H), 8.75 (d, J = 4.2 Hz, 6H), 8.81 (d, J = 4.2 Hz, 8H), 9.15 (br s, 2H), 9.61 (d, J = 4.4 Hz, 1H), 9.68−9.72 (m, 3H) ppm. ^{13}C NMR (100 MHz, $CDCl_3$, 25 °C): ^{13}C NMR (100 MHz, $CDCl_3$, 25 °C): 22.6, 90.7, 93.5, 124.4, 126.7, 126.8, 127.8, 128.2, 129.5, 130.8, 132.8, 133.2, 134.3, 134.8, 135.3, 137.1, 140.5, 142.3, 142.8, 143.6, 145.4, 146.9, 147.3, 149.5, 150.2, 151.2, 153.4 ppm. ES-MS: $C_{240}H_{157}N_{17}OS_2Zn_3$ calcd avg mass 3555.2, obsd *m*/*z* 3555.3 [M$^+$, 25]. Anal. Calcd C, 81.08; H, 4.45; N, 6.70; S, 1.80. Found: C, 81.22; H, 4.62; N, 6.88; S, 1.98.

$(ZnN_4)_3-N_3S-N_2S_2$ Porphyrin Pentad 3. Coupling of tetrad **16a** (10.0 mg, 3.46 μmol) and 5-(4-iodophenyl)-10,15,20-tri(*p*-tolyl)-21,23-dithiaporphyrin **20** (2.83 mg, 3.46 μmol) in dry toluene/triethylamine (3:1, 30 mL) in the presence of $AsPh_3$ (1.28 mg, 4.18 μmol) and $Pd_2(dba)_3$ (0.48 mg, 0.52 μmol) at 35 °C for 10 h followed by slica gel column chromatographic purification using dichloromethane/methanol (97:3) afforded the desired pentad **3** as a violet solid in 40% yield (5 mg). ^{1}H NMR (400 MHz, $CDCl_3$, 25 °C): δ = −2.69 (brs, 1H), 2.74 (s, 36H), 7.30−7.38 (m, 24H), 7.53 (d, J = 8.0 Hz, 8H), 7.58−7.64 (m, 10H), 7.80−7.84 (m, 4H), 7.89 (d, J = 8.0 Hz, 4H), 7.92−7.97 (m, 6H), 8.05−8.09 (m, 8H), 8.10−8.17 (m, 12H), 8.22 (d, J = 8.0 Hz, 4H), 8.60−8.66 (m, 8H), 8.64−8.72 (m, 10H), 8.76 (d, J = 4.4 Hz, 6 H), 8.82 (d, J = 4.4 Hz, 6 H), 8.93−8.96 (m, 4 H), 9.62 (d, J = 4.6 Hz, 1 H), 9.68−9.72 (m, 4 H), 9.77 (d, J = 4.6 Hz, 1 H) ppm. ^{13}C NMR (100 MHz, $CDCl_3$, 25 °C): δ = 21.4, 31.4, 81.8, 91.0, 123.9, 127.3, 127.4, 128.2, 128.9, 131.3, 132.6, 134.1, 134.3, 135.7, 136.5, 137.5, 137.9, 139.1, 141.1, 144.1, 147.3, 152.7, 154.5 ppm. Anal. Calcd: C, 80.71; H, 4.43; N, 6.67; S, 2.69. Found: C, 80.62; H, 4.58; N, 6.48; S, 2.84.

$(ZnN_4)_3-N_2S_2-N_2S_2$ Porphyrin Pentad 4. Samples of **17a** (10.0 mg, 3.44 μmol) and 5-(4-iodophenyl)-10,15,20-tri(2-furyl)-21,23-dithiaporphyrin **20** (2.81 mg, 3.44 μmol) were coupled in dry toluene/triethylamine (3:1, 15 mL) in the presence of a catalytic amount of $AsPh_3$ (1.26 mg, 4.12 μmol) and $Pd_2(dba)_3$ (0.47 mg, 0.51 μmol) at 35 °C under nitrogen for 10 h. The crude compound was purified by silica gel column chromatography using dichloromethane/methanol (96:4) and afforded pure pentad **4** in 45% yield (5 mg). Mp > 300 °C. IR (KBr film): ν = 3342, 3056, 3034, 2930, 2859, 2111, 1455, 992, 756 cm^{-1}. ^{1}H NMR (400 MHz, $CDCl_3$, 25 °C): δ = 2.73 (s, 27 H), 7.02−7.06 (m, 3H), 7.38−7.44 (m, 10H), 7.52−7.60 (m, 12H), 7.60−7.68 (m, 6H), 7.70−7.82 (m, 11H), 7.86−8.00 (m, 11H), 8.08−8.26 (m, 24H), 8.78−8.81 (m, 2H), 8.95−9.00 (m, 22H), 9.58−9.72 (m, 5H), 10.02−10.11 (m, 3H) ppm. ^{13}C NMR (100 MHz, $CDCl_3$, 25 °C): δ = 21.8, 31.6, 82.7, 91.8, 124.6, 127.1, 127.7, 128.4, 128.9, 131.4, 132.8, 134.8, 134.6, 135.8, 136.9, 137.2, 137.8, 140.1, 141.2, 144.6, 147.8, 152.9, 154.6 ppm. ES-MS: $C_{231}H_{144}N_{16}O_3S_4Zn_3$ calcd avg mass 3516.2, obsd *m*/*z* 3515.0 [M$^+$ − H, 25]. Anal. Calcd: C, 78.91; H, 4.13; N, 6.37; S, 3.65. Found: C, 78.86; H, 4.22; N, 6.28; S, 3.52.

Acknowledgment. We thank BRNS, CSIR, and DST for financial support.

Supporting Information Available: Experimental for compounds **5**−**17** and copies of ES-MS and ^{1}H NMR spectra of selected compounds. This material is available free of charge via the Internet at http://pubs.acs.org.

JO801455W